

TSC Spectra

Point- versus Cluster-Defects

E. Fretwurst, E. Donegani, E. Garutti, R. Klanner

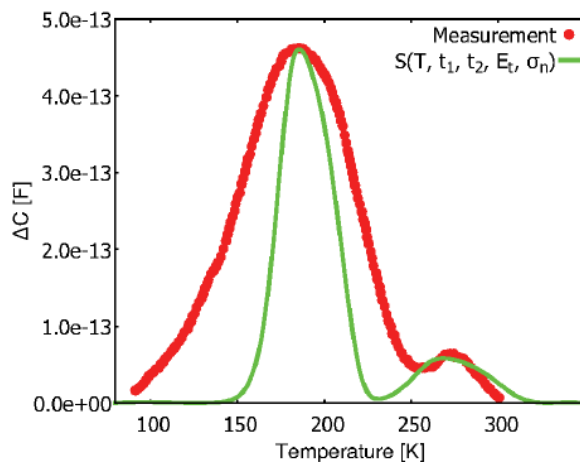
Institute for Experimental Physics
University of Hamburg

Introduction

- The peak shape of cluster-related defects recorded by TSC or DLTS differs significantly from those of point-like defects.
Main effect: The measured peaks are broader compared to point-defects.
- Such problems were studied by A. Scheinermann and A. Schenk e.g. on dislocation loops (DLs) in CMOS devices.

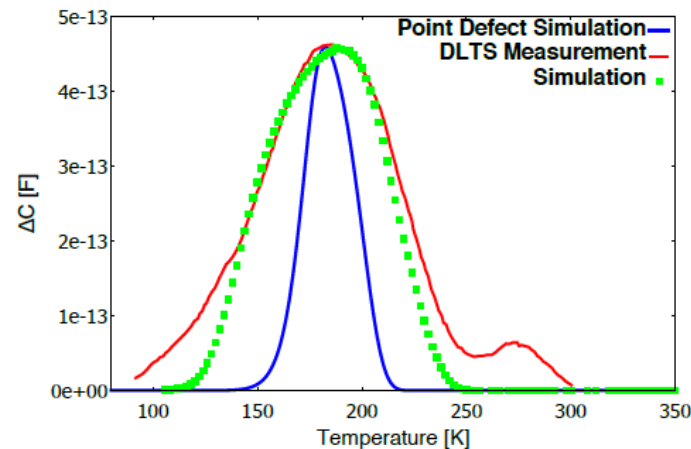
[A. Scheinermann, A. Schenk, *Phys. Status Solidi A* 211, No. 1, 136-142 (2014)]

Point defect



DLTS spectrum of DL compared with analytical theory for point defect:
 $E_t = E_C - 0.35 \text{ eV}$, $\sigma_n = 10^{-15} \text{ cm}^2$

Cluster defect



DLTS simulation of DL taking into account the Coulomb repulsion energy to the defect level at $E_t = E_C - 0.4 \text{ eV}$ and $\sigma_n = 10^{-15} \text{ cm}^2$.

Model

- **Model:**

Cluster → accumulation of point defects

→ change of local potential depending on fraction of filled states

→ activation energy E_a of defect depends on occupation → time (and T)

Example:

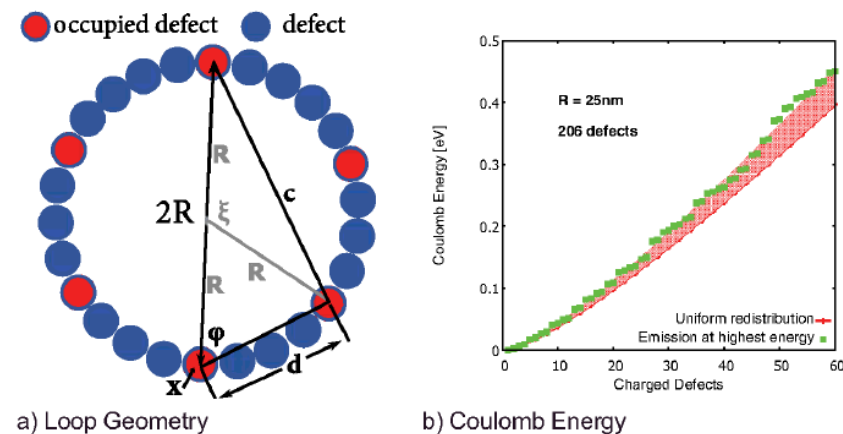
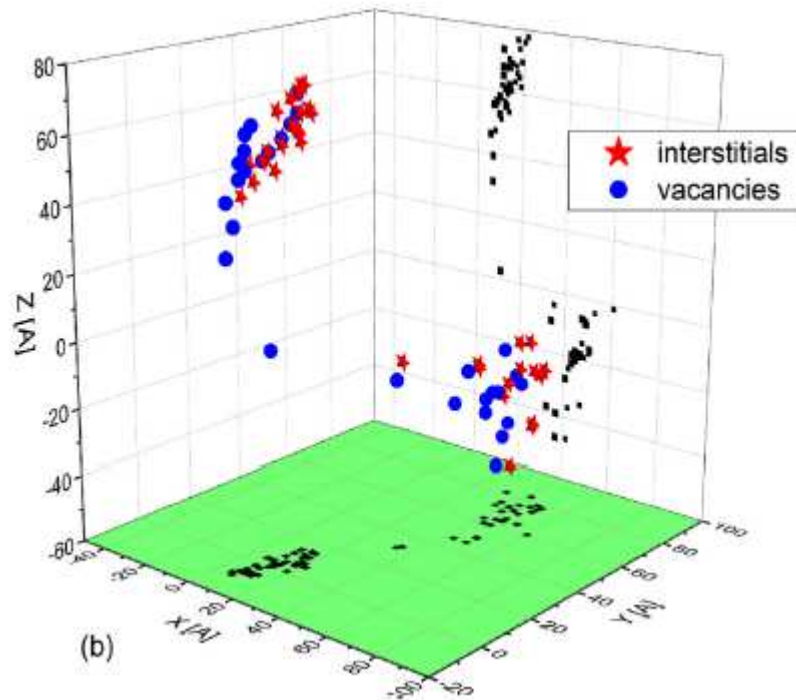


Figure 2 (a) Schematic view of DL periphery partially occupied by captured carriers with geometry used to derive the Coulomb contribution to the defect level. (b) Deviations between the assumption that captured carriers can redistribute instantaneously along the dislocation loop (solid line) and the case where they are bound to their site while capture and emission probabilities vary along the periphery of the defect with the local Coulomb energy contribution (square symbols). The shaded area indicates 15% difference from the original analytical expression.

[A. Scheinemann, A. Schenk, *Phys. Status Solidi A* 211, No. 1, 136-142 (2014)]

Model

TCAS simulation of a collision cascade for a 20 keV PKA after recombination of close Frenkel pairs.

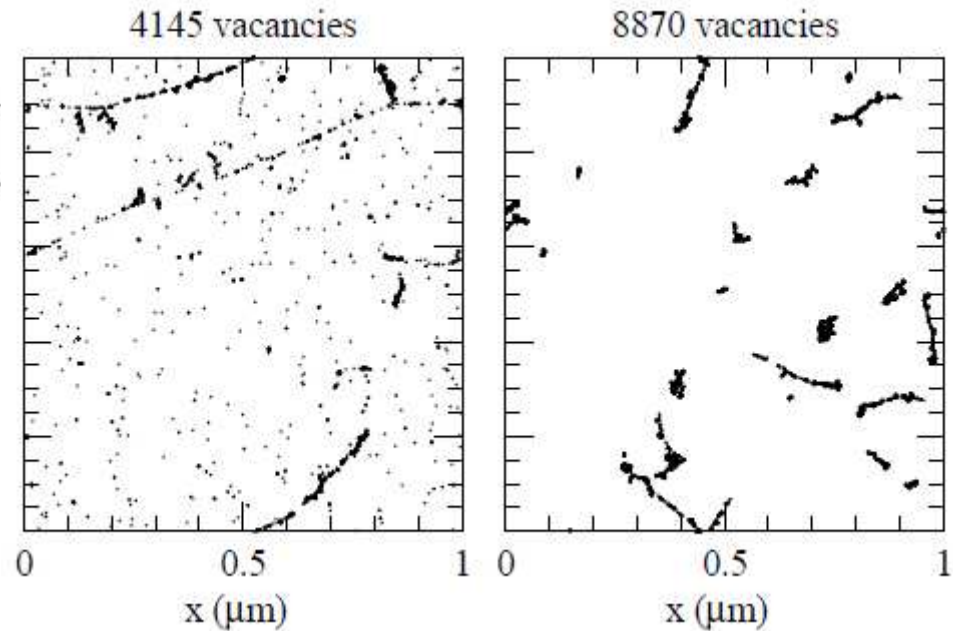


R. Radu et al., JAP 117, 164503 (2015)

Initial distribution of vacancies after $\Phi_{eq} = 10^{14} \text{ cm}^{-2}$

24 GeV/c protons

1 MeV neutrons



M. Huhtinen, NIM A 491 (2002) 194

→ distribution of vacancies (interstitials) approx. straight line.

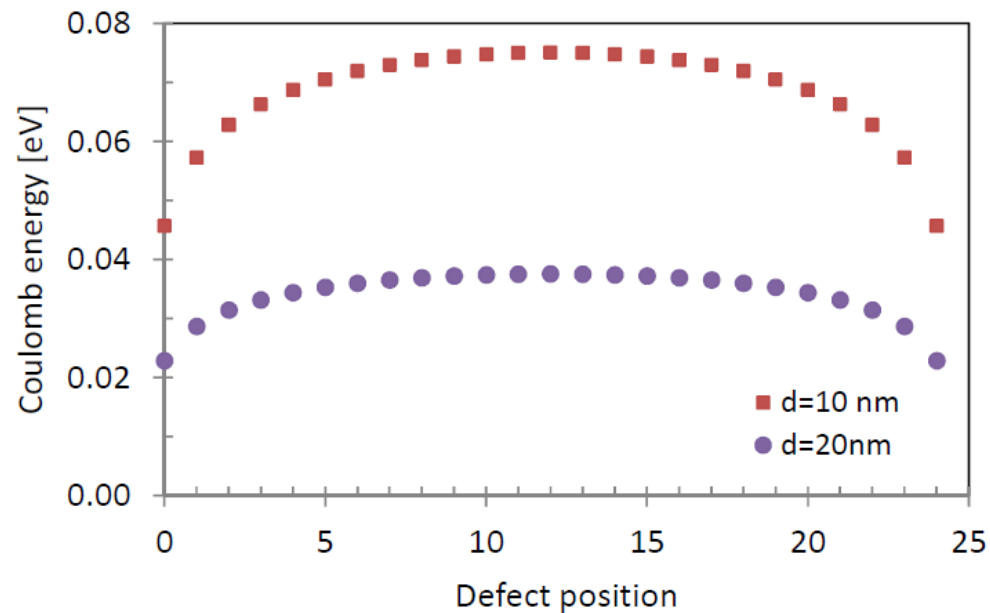
Model

Assume: n uniformly spaced point defects on a straight line,
deep acceptors, negatively charged

→ Coulomb repulsion

Energy scale:
$$E_C = \frac{q_0}{4\pi \cdot \epsilon_S \cdot \epsilon_0 d} = 0.121 \text{ eV} / d[\text{nm}]$$

Example: n = 25 (arbitrary), distance between 2 charged defects d = 10/20 nm



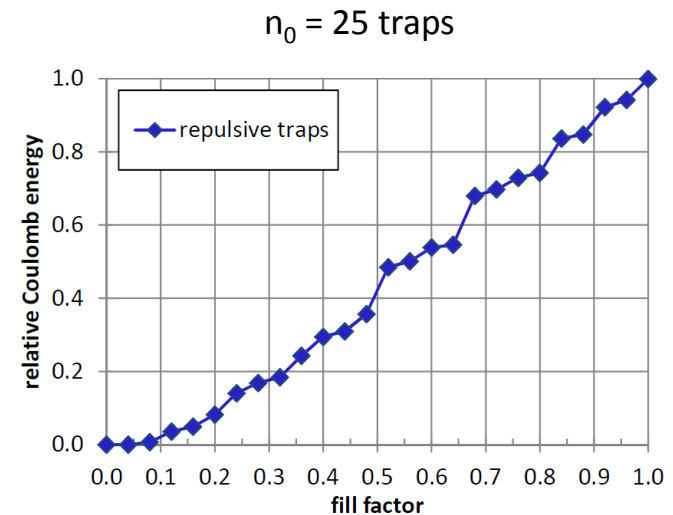
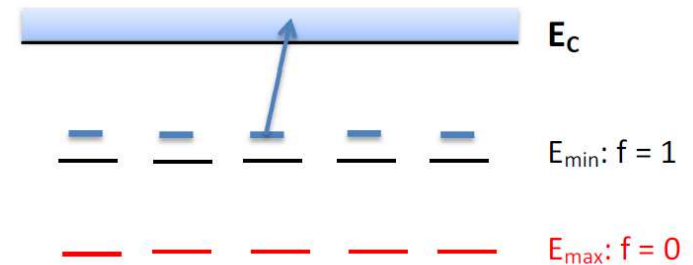
Model

Procedure:

All n defect states occupied \rightarrow calculate Coulomb energy $E_C(n) \rightarrow E_a^*(n) = E_a - E_C(n) = E_{\min}$;
fill factor $f = n/n_0 = 1$

- carrier with the highest energy is emitted
 $\rightarrow E_a^*(n-1) = E_a - E_C(n-1)$; $f = (n-1)/n_0$
- New E_C for every left carrier
 \rightarrow carrier with highest E_C emitted $\rightarrow E_a^*(n-2)$
- Successive calculation of $E_C(i)$ until last carrier emitted $\rightarrow E_C(0) = 0 \rightarrow E_a^*(0) = E_a = E_{\max}$; $f=0$

➤ $E_a^*(f)$ is approximately linear in f ,
 \approx independent of the topology of the cluster
(not shown here)



TSC model for cluster-defects

Implement $E_a^*(f)$ in TSC calculation, e.g. for an acceptor trap:

TSCurrent:
$$I(T) = \frac{1}{2} \cdot q_0 \cdot A \cdot d \cdot e_n \cdot n_t(T)$$

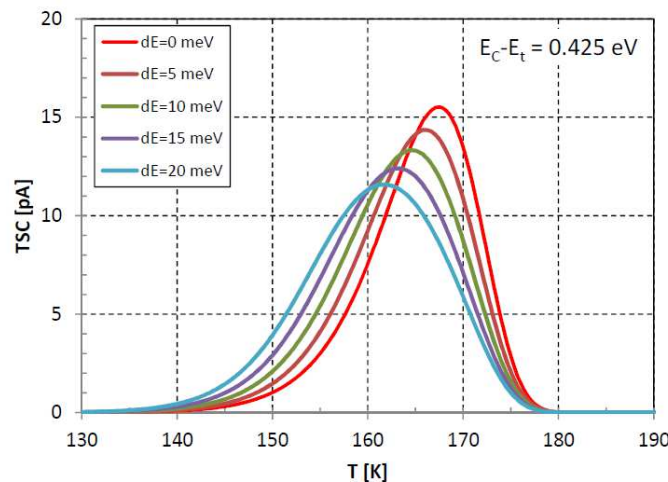
Occupied traps:
$$n_t(T) = n_{t,0} \cdot \exp\left(-\frac{\int_{T_0}^T e_n(T') dT'}{\beta}\right); \quad \beta = \text{heating rate}$$

Occupied fraction:
$$f(T) = \frac{n_t(T)}{n_{t,0}}$$

Emission rate:
$$e_n(T) = \sigma_n \cdot v_{th,n}(T) \cdot N_C(T) \cdot \exp\left(-\frac{E_a^*(f(T))}{k_B T}\right)$$

Effective energy:
$$E_a^*(f(T)) = E_{max} - (E_{max} - E_{min}) \cdot f(T)$$

Example:



$$dE = E_{max} - E_{min}$$

The T-dependence of the effective energy E_a^* via $f(T)$ leads to a **shift** and **broadening** of the TSC-peak

Application to proton irradiated diode

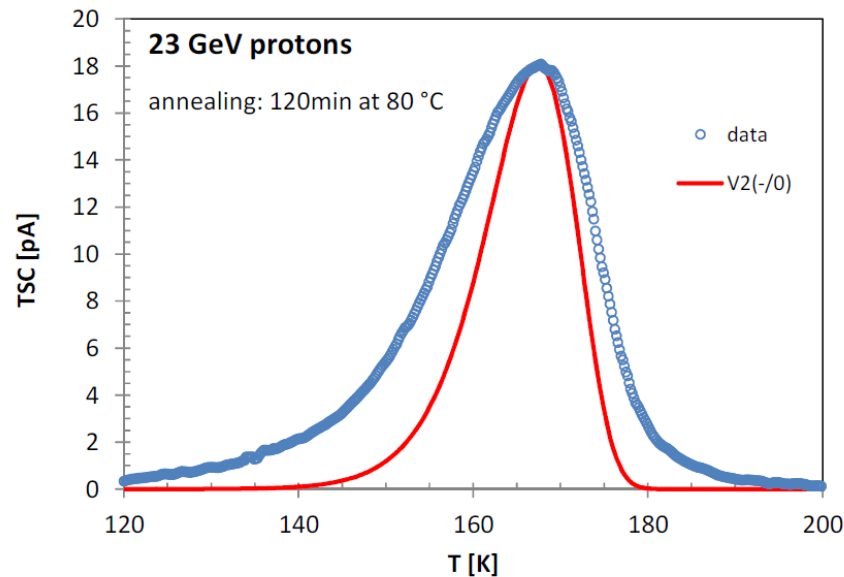
Diode: Standard EPI, n-type, 75 μm thick

Irradiation: 24 GeV/c protons, $\Phi_{\text{eq}} = 1 \times 10^{13} \text{ cm}^{-2}$

TSC spectrum: cooling: $V_c = 0 \text{ V}$, filling: $V_f = 0 \text{ V}$, heating: reverse bias $V_R = 150 \text{ V}$

→ only electron traps are filled.

Standard theory: point defect



Assumed defect: $V_2(-/0)$

Activation energy:

$$E_a = E_C - E_t = 0.425 \text{ eV}$$

Capture cross-section:

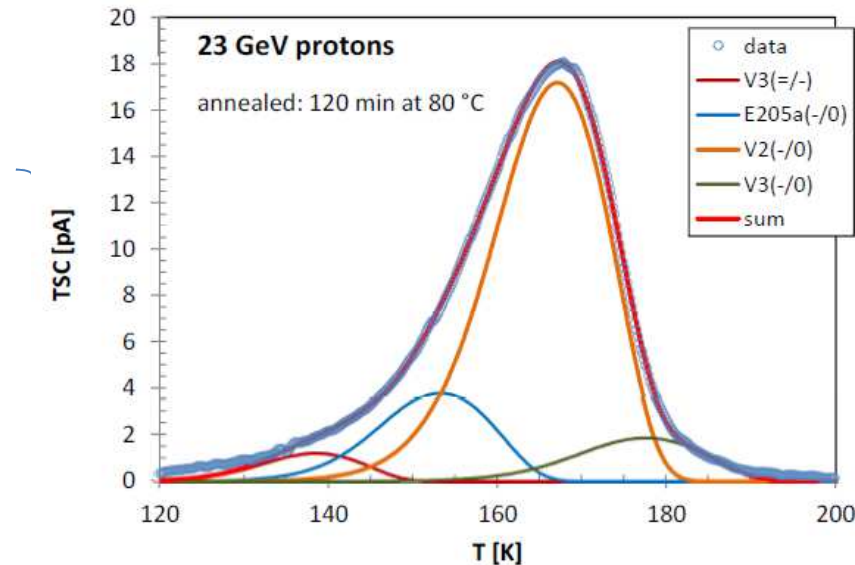
$$\sigma_n = 8.3 \cdot 10^{-16} \text{ cm}^2$$

➤ TSC peak cannot be described by a single level point defect, but

Application to proton irradiated diode

Diode: Standard EPI, n-type, 75 μm thick

Irradiation: 24 GeV/c protons, $\Phi_{\text{eq}} = 1 \times 10^{13} \text{ cm}^{-2}$, annealing: 120 min at 80 °C



TSC model:

4 cluster defects

$$E_a^* = E_a - \Delta E \cdot f$$

$$\Delta E = E_{\text{max}} - E_{\text{min}}$$

$$E_a = E_{\text{max}} \text{ from literature}$$

Defect	E_a [eV]	ΔE [meV]	σ_n [cm^2]	N_t [cm^{-3}]
$V_3(=/-)$	0.359	14.0	$1.5 \cdot 10^{-15}$	$6.8 \cdot 10^{11}$
E205a	0.393	15.9	$7.8 \cdot 10^{-16}$	$2.4 \cdot 10^{12}$
$V_2(-/0)$	0.425	13.0	$6.0 \cdot 10^{-16}$	$1.1 \cdot 10^{13}$
$V_3(-/0)$	0.460	16.8	$7.3 \cdot 10^{-16}$	$1.3 \cdot 10^{12}$

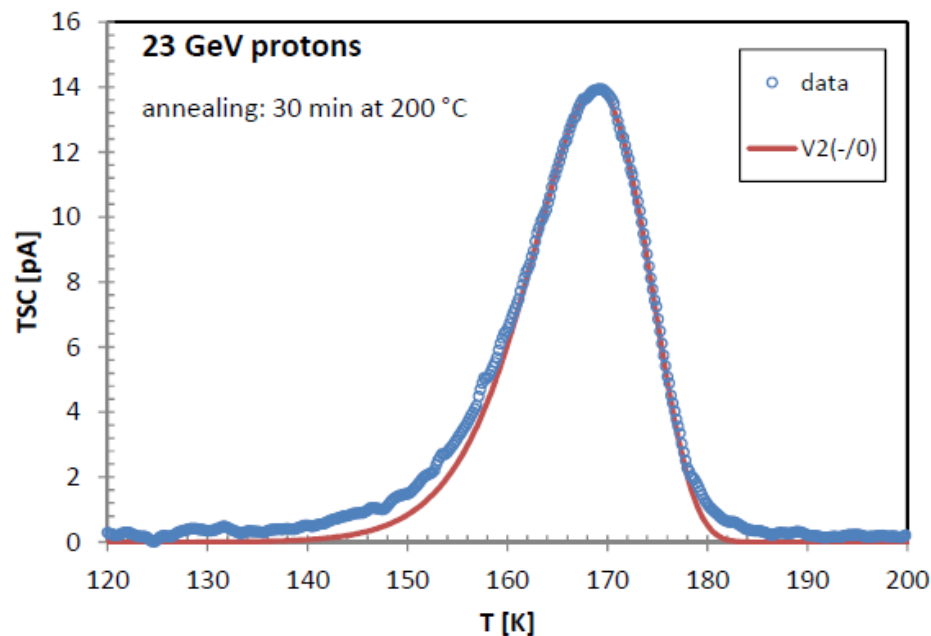
Attention:

Parameter ΔE and σ_n are strongly correlated, E_a fixed

Application to proton irradiated diode

Diode: Standard EPI, n-type, 75 μm thick

Irradiation: 24 GeV/c protons, $\Phi_{\text{eq}} = 1 \times 10^{13} \text{ cm}^{-2}$, annealing: 30 min at 200 $^{\circ}\text{C}$



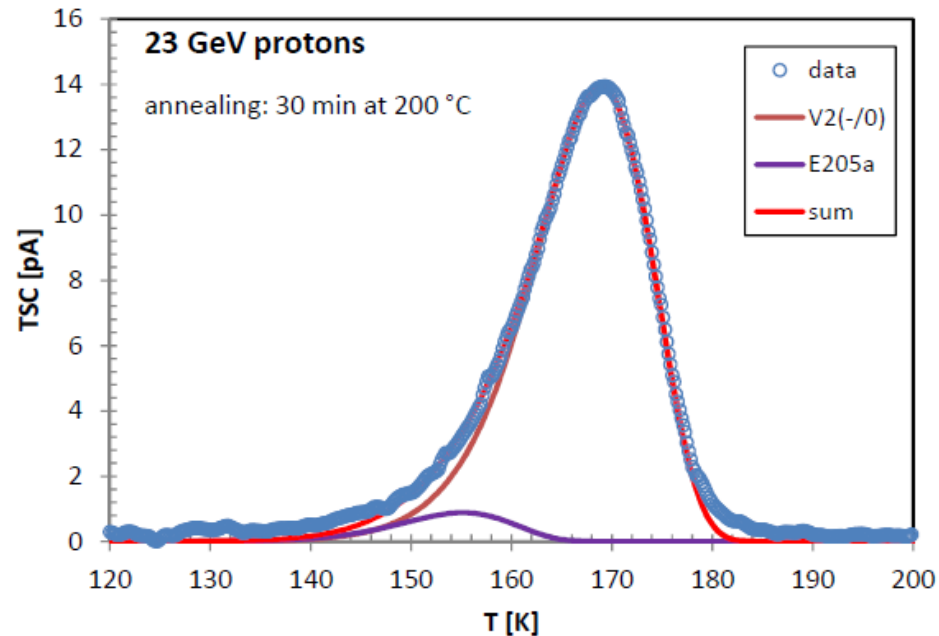
TSC model:
1 cluster defects;
 $V_2(-/0)$
low T-tail not reproduced

Defect	E_a [eV]	ΔE [meV]	σ_n [cm^2]	N_t [cm^{-3}]
$V_2(-/0)$	0.425	4.5	$6.8 \cdot 10^{-16}$	$7.9 \cdot 10^{12}$

Application to proton irradiated diode

Diode: Standard EPI, n-type, 75 μm thick

Irradiation: 24 GeV/c protons, $\Phi_{\text{eq}} = 1 \times 10^{13} \text{ cm}^{-2}$, annealing: 30 min at 200 °C



TSC model:

2 cluster defects;
 $V_2(-/0)$, E205a

Much smaller ΔE
 compared to 80 °C
 120 min annealing.

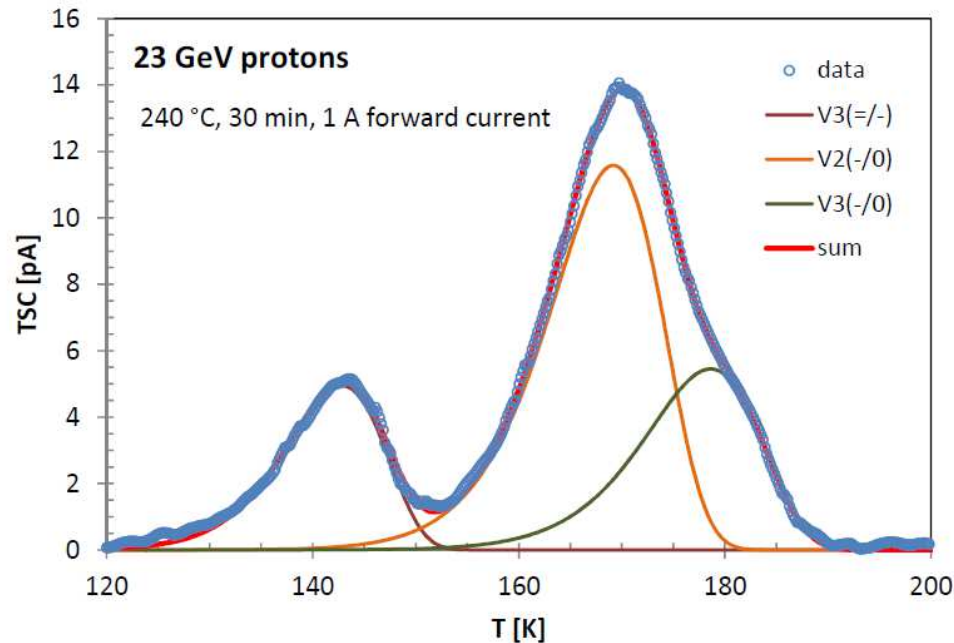
Cluster-effect after 200 °C
 strongly reduced.

Defect	E_a [eV]	ΔE [meV]	σ_n [cm^2]	N_t [cm^{-3}]
E205a	0.393	6.3	$9.4 \cdot 10^{-16}$	$4.8 \cdot 10^{11}$
$V_2(-/0)$	0.425	4.5	$6.8 \cdot 10^{-16}$	$7.9 \cdot 10^{12}$

Application to proton irradiated diode

Diode: Standard EPI, n-type, 75 μm thick

Irradiation: 24 GeV/c protons, $\Phi_{\text{eq}} = 1 \times 10^{13} \text{ cm}^{-2}$, annealing: 30 min at 240 °C



TSC model:

3 defects,

$V_3(=/-)$, $V_2(-/0)$, $V_3(-/0)$

V_3 defect partly recovered by injection of 1A forward current.

All 3 defects are more point-like defects.

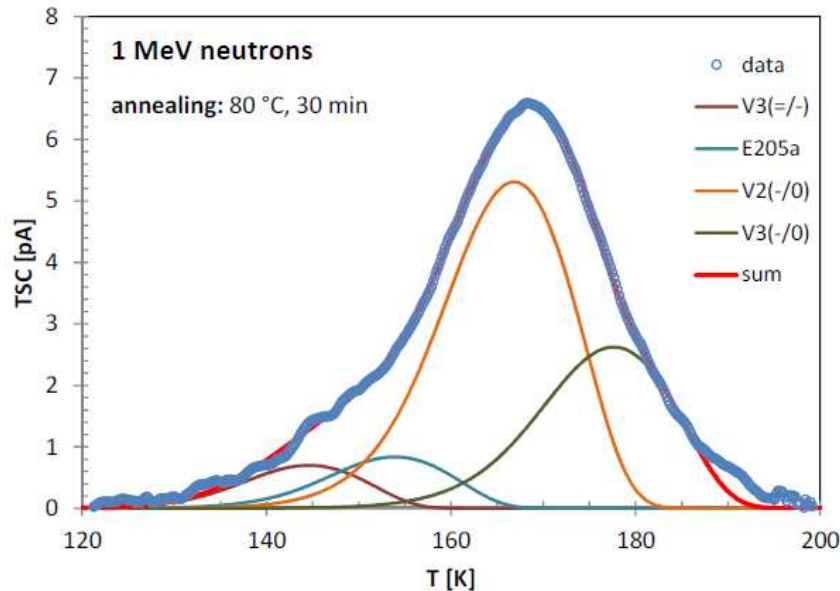
Clustering nearly vanished.

Defect	E_a [eV]	ΔE [meV]	σ_n [cm^2]	N_t [cm^{-3}]
$V_3(=/-)$	0.359	3.0	$1.4 \cdot 10^{-15}$	$2.3 \cdot 10^{12}$
$V_2(-/0)$	0.425	1.3	$7.3 \cdot 10^{-16}$	$6.2 \cdot 10^{12}$
$V_3(-/0)$	0.460	1.6	$1.4 \cdot 10^{-15}$	$3.0 \cdot 10^{12}$

Application to neutron irradiated diode

Diode: EPI-DO, n-type, 75 μm thick

Irradiation: 1 MeV neutrons, $\Phi_{\text{eq}} = 5 \times 10^{13} \text{ cm}^{-2}$, annealing: 30 min at 80 °C



TSC model:
4 cluster-defects

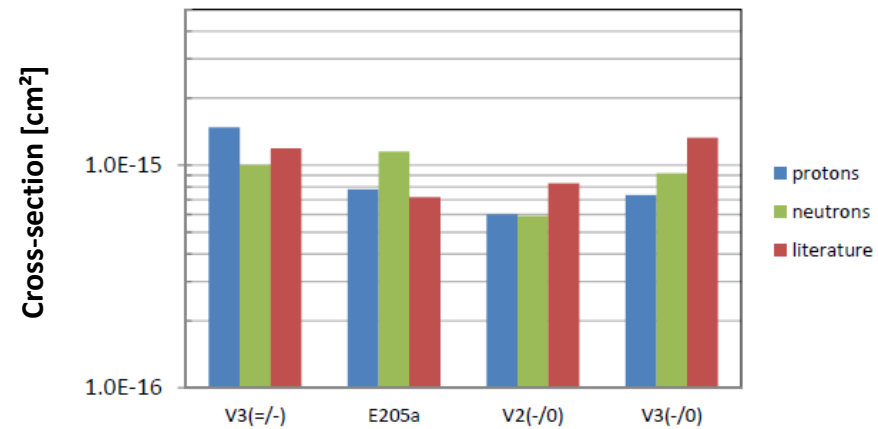
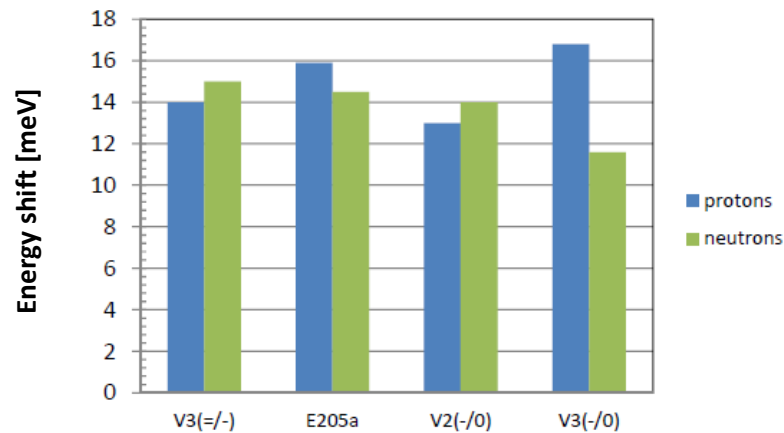
ΔE comparable with proton irradiated device.

Cluster-effect for GeV protons \approx for neutrons

Defect	E_a [eV]	ΔE [meV]	σ_n [cm^2]	N_t [cm^{-3}]
$V_3(=/-)$	0.359	15.0	$1.0 \cdot 10^{-15}$	$6.8 \cdot 10^{11}$
E205a	0.393	14.5	$1.2 \cdot 10^{-15}$	$5.3 \cdot 10^{11}$
$V_2(-/0)$	0.425	14.0	$5.9 \cdot 10^{-16}$	$3.6 \cdot 10^{12}$
$V_3(-/0)$	0.460	11.6	$9.2 \cdot 10^{-16}$	$1.8 \cdot 10^{12}$

Comparison protons versus neutrons

Comparison of ΔE and σ_n for the different cluster-defects induced by GeV protons and neutrons and after annealing at 80 °C



ΔE for proton irradiated silicon comparable with results for neutrons

Overall:

$$\langle \Delta E \rangle = (14.4 + 2.5 / - 2.8) \text{ meV,}$$

Deviation dominated by values for $V_3(-/0)$

Variation of σ_n for proton and neutron irradiated devices $\approx +32\%$ to -48%

Ratio to literature values:

$$\text{Protons: } \sigma_n^{(\text{literature})} / \sigma_n^{(\text{proton})} \approx 0.8 - 1.8$$

$$\text{Neutrons: } \sigma_n^{(\text{literature})} / \sigma_n^{(\text{neutron})} \approx 0.6 - 1.4$$

Literature values from DLTS studies

No big difference in cluster-effect between GeV protons and neutrons

Conclusions/Comments

- Observed TSC peak shifts and broadening for acceptor-like cluster-defects can be described by the **Coulomb repulsion model**.
- Change of the activation energy ΔE is in the order of 14 meV independent of damaging hadron (GeV proton or MeV neutron) after annealing at 80 °C.
- ΔE decreases with annealing \rightarrow cluster-effect decreases (cluster size?, density of defects?)
- Consequences of the model for the electrical properties of sensors (dark current, space charge and charge collection) has to be studied.
- Can the model be implemented in TCAD-simulations?

There are several assumptions in the Coulomb interaction model:

- No redistribution of the trapped charges to an equidistant situation after each charge emission
- The linear dependence of $E_c(f)$ in the occupation is a rough approximation which might not be the reality in radiation-induced clusters by hadrons; e.g. statistically distributed defects in the disordered regions, disordered region of different size.

Other possible reasons for broadening of DLTS or TSC peaks:

- Energy band around defect levels due to strain field in the disordered region
- Defect level coupling due to interaction between the closely spaced defects
 \rightarrow also called “inter-defect charge exchange”

This effect seems to be unlikely as concluded in the publication of A. Scheinemann and A. Schenk.

BACK UP

Estimation of Cluster Size

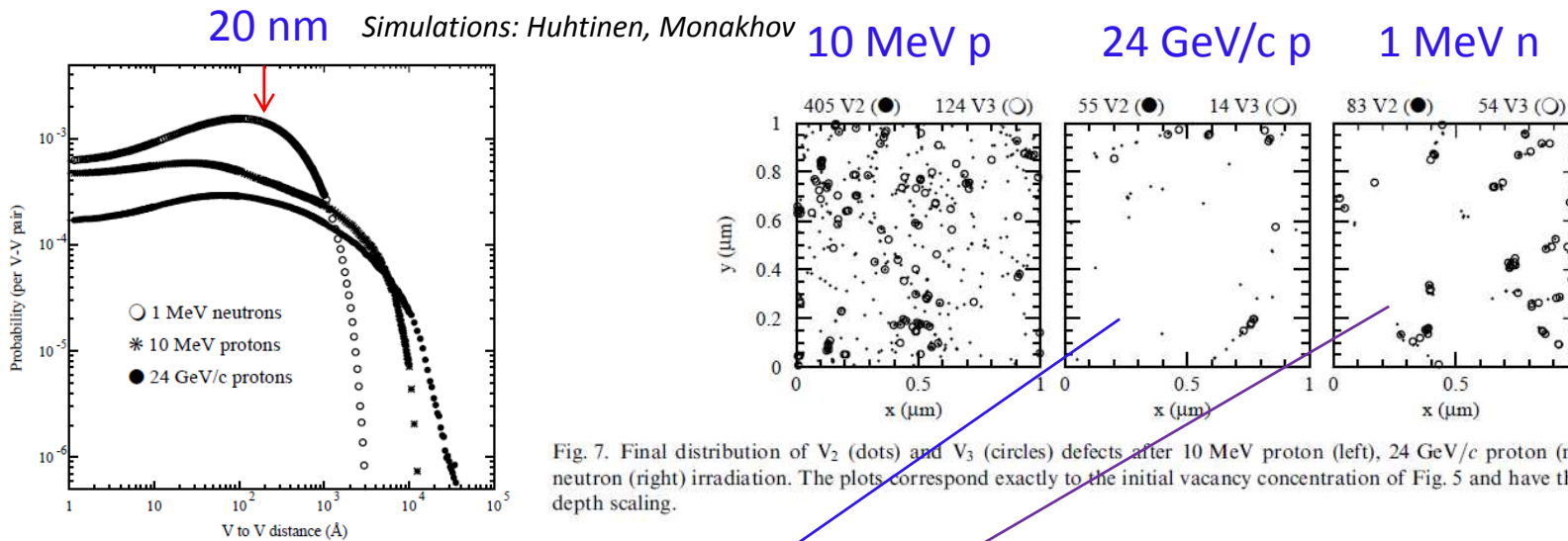


Fig. 6. Probability distribution of vacancy–vacancy distances within a single event. The plot represents an average over many thousand events.

Average V_2 distance:

24 GeV/c protons $\langle d \rangle \approx 18$ nm

1 MeV neutrons $\langle d \rangle \approx 12$ nm

Cluster length $l \approx 100$ nm

Lateral extension $r \approx 25$ nm

Volume $V \approx 2 \cdot 10^{-16}$ cm³,

Number of V_2 defects in cluster ≈ 5

→ concentration $[V_2] \approx 2.5 \cdot 10^{16}$ cm⁻³

Fig. 7. Final distribution of V_2 (dots) and V_3 (circles) defects after 10 MeV proton (left), 24 GeV/c proton (middle) and 1 MeV neutron (right) irradiation. The plots correspond exactly to the initial vacancy concentration of Fig. 5 and have the same fluence and depth scaling.

